

Interaction of the Aromatics Tyr-72/Trp-288 in the Interface of the Extracellular and Transmembrane Domains Is Essential for Proton Gating of Acid-sensing Ion Channels*

Received for publication, July 11, 2008, and in revised form, December 8, 2008. Published, JBC Papers in Press, December 11, 2008, DOI 10.1074/jbc.M805302200

Tianbo Li, Youshan Yang, and Cecilia M. Canessa¹

From the Department of Cellular and Molecular Physiology, Yale University, New Haven, Connecticut 06520-8026

Acid-sensing ion channels are proton-activated ion channels expressed in the nervous system. They belong to the family of ENaC/Degenerins whose members share a conserved structure but are activated by widely diverse stimuli. We show that interaction of two aromatic residues, Tyr-72, located immediately after the first transmembrane segment, and Trp-288, located at the tip of a loop of the extracellular domain directed toward the first transmembrane segment, is essential for proton activation of the acid-sensing ion channels. The subdomain containing Trp-288 is a module tethered to the rest of the extracellular domain by short linkers and intrasubunit interactions between residues in the putative "proton sensor." Mutations in these two areas shift the apparent affinity of protons toward a more acidic range and change the kinetics of activation and desensitization. These results are consistent with displacement of the module relative to the rest of the extracellular domain to allow interaction of Trp-288 with Tyr-72 during gating. We propose that such interaction may provide functional coupling between the extracellular domain and the pore domain.

The acid-sensing ion channels (ASICs)² are voltage-insensitive sodium channels turned on and off by extracellular protons. Four ASIC genes in the human genome, ASIC1 to ASIC4, give rise to at least six isoforms that associate in various combinations to form channels with different functional properties (1, 2). The ASICs constitute a distinct group in the large family of channels known as Degenerins characterized by a common structure but widely diverse gating stimuli: mechanical forces (3), neuropeptides (4, 5), protons (6), or no stimulus at all, such as ENaC, which exhibits constitutive activity (7). The structure shared by all Degenerins consists of two transmembrane segments, TM1 and TM2, a large extracellular domain, and short cytoplasmic amino and carboxyl termini. The recently pub-

lished crystal structure of a truncated chicken ASIC1 (cASIC1) at a resolution of 1.9 Å (8) shows that ASIC1 is a trimer, and it provides detailed structure of the large extracellular domain that is crucial for understanding the gating mechanism of the ASICs. A feature revealed by the atomic structure is a cluster of negatively and one positively charged residue in the interface of subdomain D (Arg-191), subdomain E (Asp-238 and Glu-239), and subdomain F (Asp-346 and Asp-350) (see Fig. 1A) that was hypothesized to constitute the proton sensor. Furthermore, it was proposed that binding of protons to this site displaces subdomain F toward TM1 to open the pore (8).

Although the solved atomic structure of cASIC1 provides a valuable tool to advance the understanding of how external protons activate the ASICs, it represents only a snapshot of the gating process thereby additional experimental evidence is needed to elucidate the gating mechanism. The general idea that conformational changes triggered by binding of the specific agonist to the extracellular domain of a ligand activated channel need to be transmitted to the transmembrane domain, where the pore gate is located, draws attention to the pair of closely located residues, Tyr-72 and Trp-288, as they provide a potential contact site between the extracellular and the transmembrane domains.

This study examines the functional role of the conserved residues, Tyr-72 and Trp-288, that are located distantly in the primary sequence but are brought to close proximity (~3.7 Å) by the folding of the extracellular domain (ECD). This arrangement could provide a contact site between the ECD and TM1 whereby a conformation change of the ECD is transmitted to the pore gate in the transmembrane domain.

EXPERIMENTAL PROCEDURES

Electrophysiology and Two-electrode Voltage Clamp of Oocytes—Xenopus laevis oocytes were injected with 5 ng of cRNA in a volume of 50 nl and used after 2–4 days of incubation at 16 °C. For two-electrode voltage clamp experiments, oocytes were placed in a recording chamber (400 μl) perfused by gravity at a rate of 4 ml/min. Oocytes were impaled with two glass microelectrodes filled with 3 M KCl having a resistance lower than 1 megaohm. Membrane potential was held at –60 mV, and whole-cell currents were recorded with a Clamp OC-725B (Warner Instrument Corp., Hamden, CT) and digitized at a sampling rate of 2 kHz (PowerLab/200, ADInstruments). Composition of the standard bath solution was 120 mM NaCl, 3 mM KCl, 2 mM CaCl₂, 10 mM HEPES-MES adjusted to pH 7.4. Activating solutions were administered by a perfusion system posi-

* This work was supported, in whole or in part, by National Institutes of Health Grant DK544602 (NIDDK). This work was also supported by American Heart Association Grant-in-aid R06523 (to C. M. C.). The costs of publication of this article were defrayed in part by the payment of page charges. This article must therefore be hereby marked "advertisement" in accordance with 18 U.S.C. Section 1734 solely to indicate this fact.

⌘ Author's Choice—Final version full access.

¹ To whom correspondence should be addressed: Dept. of Cellular and Molecular Physiology, Yale University, 333 Cedar St., New Haven, CT 06520-8026. Tel.: 203-785-5892; Fax: 203-785-4951; E-mail: Cecilia.canessa@yale.edu.

² The abbreviations used are: ASIC, acid-sensing ion channel; cASIC, chicken ASIC; rASIC, rat ASIC; ECD, extracellular domain; MES, 4-morpholineethanesulfonic acid; WT, wild type.

Tyr-72 and Trp-288 Are Required for ASIC Function

tioned directly in front of the oocyte. Composition of activating solutions was 120 mM NaCl, 2 mM KCl, 1 mM CaCl₂, 10 mM HEPES-MES or 10 mM MES adjusted to pH 7.2–4.0.

Patch Clamp—Currents from outside-out patches were recorded with an EPC-9 amplifier and the Pulse acquisition program (HEKA Electronic). Patch pipettes were pulled from PG150T glass (Warner Instruments) to tip diameters of 2–5 μm after heat polishing. Bath solution for patch clamp recording was 120 mM NaCl, 3 mM KCl, 2 mM CaCl₂, and 10 mM HEPES adjusted to pH 7.4. The pipette solution was of identical composition as the bath, but it did not contain CaCl₂. Activating solutions were buffered with MES to pH 7.2, 7.0, 6.5, 6.0, 5.0, or 4.0. Application of activation solutions was performed using the SF 77A Perfusion Fast-Step device (Warner Instruments) under control of the program Pulse.

Calculation of Apparent p*H*₅₀—Oocytes were exposed sequentially to solutions of decreasing pH from 7.2 to 4.0. Between test applications, oocytes were perfused with solution of pH 7.4 for at least 30 s to recover from desensitization. If possible, each oocyte was tested twice with the whole range of pH solutions. The average of the peak currents from each pH was normalized to the value of pH that produced maximal current. The mean and standard deviation were obtained, and the p*H*₅₀ was calculated according to the equation $I = 1/(1 + (EC_{50}/[H])^n)$, where *I* is the normalized value for the test pH, EC₅₀ is the concentration of protons that induces half-maximal currents, and *n* is the Hill coefficient. KaleidaGraph (Synergy Software) was used to draw graphs and for curve-fitting.

Desensitization Rates—The desensitization rate was calculated by fitting the decay of proton-activated currents from outside-out patches to a single exponential.

DNA Constructs and Site-directed Mutagenesis—Rat ASIC1a cDNA was modified by the addition of a V5 tag at the carboxyl terminus. Mutations were introduced in the sequence of rASIC1a, ASIC2a, and ASIC3 and rat α, β, and γENaC subunits using QuikChange site-directed mutagenesis kit (Stratagene). All cDNAs were sequenced to confirm the presence of the mutations.

Surface Biotinylation and Western Blotting—Oocytes injected with wild type or mutant rASIC1 cRNAs were surface-biotinylated as previously described (9). Cells were homogenized in 1% Triton X-100 and cleared by centrifugation, and the biotinylated proteins were recovered with streptavidin beads (Pierce). Proteins were resolved by electrophoresis on 10% SDS-PAGE, transferred to Immobilon membranes, and processed for Western blotting with anti-V5 monoclonal antibody (Invitrogen).

RESULTS

Residues Tyr-72 and Trp-288 Are Essential for ASIC Function—The residue Tyr-72, located in the tether after TM1, and Trp-288, at the tip of the loop of subdomain F (Fig. 1*a*), are in close proximity in the crystal structure of cASIC1. Substitution of any of them by Gly in rat ASIC1 makes channels unresponsive to pH as low as 4.0. The same positions were subsequently replaced by amino acids with different side chains as indicated in Table 1. Aromatic amino acids, Y, F, W, or H and swapping of the residues to Trp-72 and Tyr-288 produced functional channels (Fig. 2*A*). By contrast, small or large aliphatic side chains,

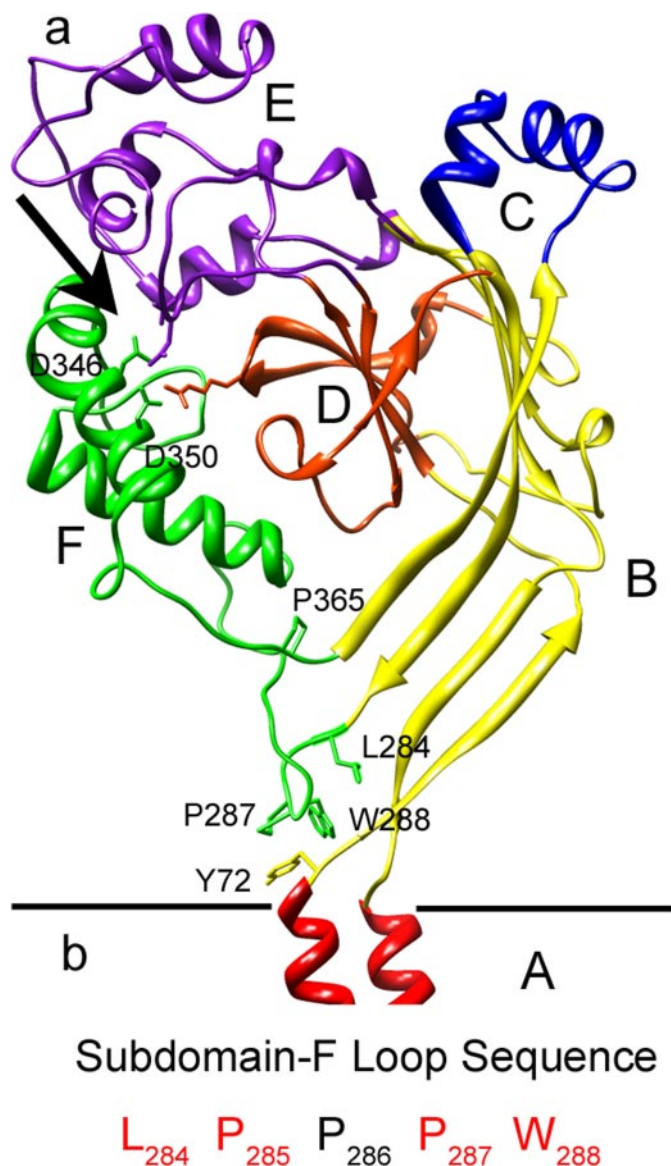


FIGURE 1. Ribbon representation of chicken ASIC1 structure. *a*, a single subunit is shown for simplicity with subdomains, A to F, indicated in different colors. The arrow points to the putative proton sensor with side chains of charged residues represented as sticks. Amino acids important for ASIC1 gating that were mutated in this study are also shown. The image was obtained with the molecular graphics program Chimera. *b*, amino acid sequence of subdomain F loop. Residues conserved in all ASIC proteins are in red.

proline, or negatively charged residues eliminated proton-induced currents. Histidine substitutions in 72 and 288 and arginine in position 72 (Y72R), but not in position 288 (W288R), retained channel function. However, all these functional mutant channels expressed lower proton sensitivity and faster desensitization rate than WT ASIC1 (Table 1 and Fig. 2). Lysine, another positively charged residue, introduced in position 72 or 288 produced channels unresponsive to pH 4.0.

The absence of ASIC1 current induced by the former mutations was not explained by intracellular retention of the mutant channels because biotinylation of surface proteins revealed equal amounts of rASIC1 protein in the plasma membrane of cells expressing wild type or mutants Gly-72 or Gly-288 as indicated by Western blotting (Fig. 2*D*).

As aromatic amino acids at positions corresponding to 72 and 288 in ASIC1 are present in other Degenerins, from *Caenorhabditis elegans* to humans, we examined whether those residues are also essential for function in other channels. Substitution of either one the aromatic residues by Ala or Gly in rat ASIC2a and ASIC3 also produced non-functional channels.

The epithelial sodium channel, ENaC, is another member of the Degenerins and is closely related in structure to the ASICs,

TABLE 1

The numbers represent the mean \pm S.D. whole-cell currents elicited by pH 6.0 of at least 10 independent oocytes

Mutant	Current	Mutant	Current
	μA		μA
WT	13 \pm 5		
Y72F	15 \pm 4	W288F	14 \pm 3
Y72W	11 \pm 6	W288Y	10 \pm 5
Y72H	4 \pm 0.6 ^a	W288H	18 \pm 5
Y72R	8 \pm 3	W288R	0
Y72K	0	W288K	0
Y72G	0	W288G	0
Y72A	0	W288A	0
Y72L	0	W288L	0
Y72V	0	W288V	0
Y72T	0	W288T	0
Y72P	0	W288P	0
Y72E	0	W288E	0
Y72C	0	Y72C/W288H	0
Y72Q	0	W288Q	0
L284A	15 \pm 4.5	Y72W/W288Y	17 \pm 6
L284P	0	Y72H/W288H	0.9 \pm 0.3 ^a
P285Q/A	14 \pm 5	Y72R/W288H	0.7 \pm 0.2 ^a
P287Q/A	0	P365A	2.6 \pm 1.5 ^a

^a $p < 0.001$, statistically significant difference compared to WT.

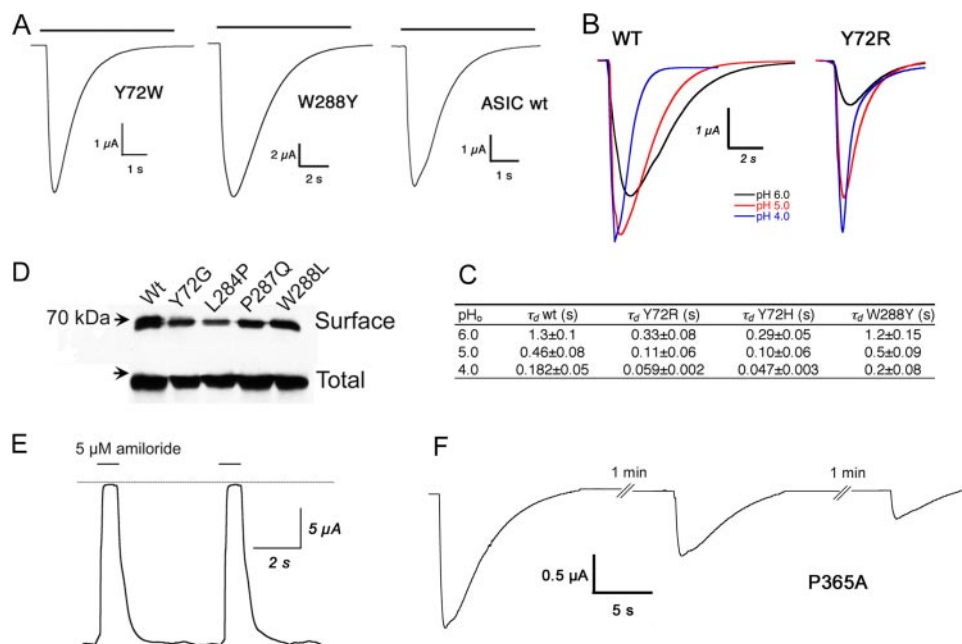


FIGURE 2. Functional effect of mutations in rat ASIC1. A, whole-cell currents of oocytes expressing wild type or mutant rASIC1 with aromatic residues in positions 72 and 288 stimulated with solution of pH 6.0. Bars above current traces indicate the duration of the test pH. B, family of currents elicited by changes in external pH of ASIC1 WT and mutant Y72R. C, table showing average values for the time constant of desensitization (τ_d) of wild type and mutants Y72R and Y72H obtained at various values of external pH (pH₀). D, Western blot analysis of surface-biotinylated and total ASIC1 proteins of wild type and nonfunctional mutants. E, representative current trace of ENaC mutant channels carrying Ala in the corresponding positions 72 and 288 of ASIC1. The dotted line indicates the zero current level, and the bars above the current trace represent application to the bath of the specific blocker amiloride. Membrane holding potential was -60 mV. Bath solution contained 120 mM NaCl, pH 7.4. F, currents of mutant ASIC1-P365A show decreased in the magnitude of the peak current, slow rates of activation and desensitization, and impaired recovery from desensitization. Time and current scales are shown with the bars below each trace.

although it differs in means of activation as ENaC is not gated by protons but is instead constitutively open. Additionally, ENaC is a heterotrimer of three different subunits α , β and γ ; each of the subunits has aromatic residues in the following positions that correspond to Tyr-72 and Trp-288 in the ASICs: α Tyr-138 and α Tyr-418, β Trp-77 and β Tyr-356, and γ Tyr-79 and γ Tyr-370. Substitution for alanine of all six aromatic residues and expression in oocytes of the double mutants α , β , and γ produced large non-desensitizing inward currents completely blocked by the specific inhibitor amiloride, wild type 22 ± 6 ($n = 12$), and mutant 26 ± 8 ($n = 12$) (Fig. 2E).

These results indicate that aromatic residues or arginine must occupy position 72, and only aromatic residues must be in position 288 to maintain proton sensitivity of the ASICs. The same pair of aromatic residues in the structurally related ENaC channel is not essential for function.

Functional Channels with Histidine or Arginine Substitutions—As indicated, all the aromatic residues Tyr, Phe, Trp, including His, at positions 72 and 288 produced channels responsive to protons, but only Tyr, Phe, and Trp maintained the functional properties of ASIC1 wild type. Substitutions by His shifted the sensitivity to protons toward more acidic pH and decreased the magnitude of the peak currents, in particular Y72H and the double mutant Y72H/W288H. The average magnitude of the peak current at pH 5.0 was 18 ± 5 , 4 ± 0.6 , and 0.9 ± 0.3 μA /oocyte for mutant channels W288H, Y72H, and Y72H/W288H, respectively (Table 1). Rates of desensitization were

in average 3-fold faster in the mutant Y72H than in WT channels. Fig. 2C shows the calculated time constant of desensitization (τ_d) obtained from multichannel patches in the outside-out configuration. The apparent pH₅₀ was 5.2 for Y72R compared with 6.6 for WT ASIC1 (Fig. 2B). We also observed a 3-fold faster desensitization rate in ASIC1- Y72R for all tested pH values (Fig. 2C).

These findings show that the imidazole ring can substitute at least in part for other canonical aromatic rings but at the expense of decreasing proton sensitivity. Also significant is the no-additive effects of His in positions 72 and 288, suggesting that these two residues may interact functionally.

Functional Interaction of Histidine Residues in Positions 72 and 288—Functional interaction between two residues can be measured by quantitatively comparing the properties of the two singly substituted proteins with that of the protein containing both mutations. If the sum of the effects of two single substitutions equals the change

Tyr-72 and Trp-288 Are Required for ASIC Function

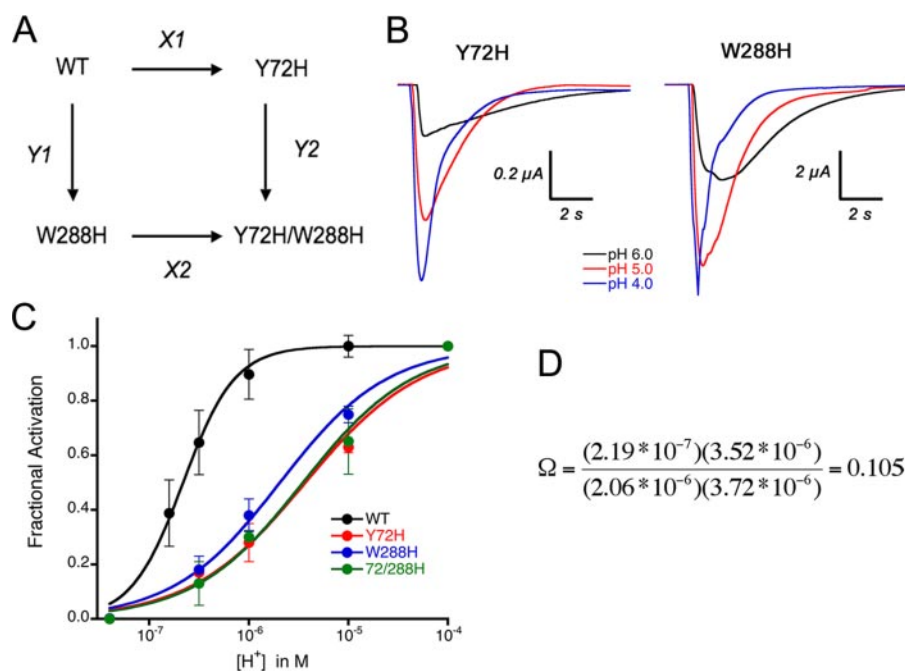


FIGURE 3. Double mutant cycle analysis of rASIC1 His mutants in positions 72 and 288. *A*, thermodynamic mutant cycle where $X1$, $X2$, $Y1$, and $Y2$ represent change in apparent proton affinity along the arrow. *B*, family of currents induced by lowering the external pH for mutant channels Y72H and W288H. *C*, proton activation curves for the channels comprising the thermodynamic mutant cycle shown in *A*. *D*, coupling coefficient Ω calculated from the apparent EC_{50} corresponding to wild type and the single and double His mutants.

seen in the double mutant, then the residues at these two positions do not interact. If the effects are not additive, the two amino acids must interact either directly or indirectly (10, 11).

Double-mutant cycle analysis is a formal way of quantifying the independence of two mutations in their effects on the function of a protein (12). The square in Fig. 3 describes the double mutant cycle relating wild type, single mutants (Y72H or W288H), and double mutant (Y72H/W288H) channels. Each arrow number represents the factor by which proton affinity changes along the direction of the arrow. For instance, $X1$ equals $EC_{50}^{WT}/EC_{50}^{Y72H}$. The affinity change in going from WT to double mutant must be the same regardless of the pathway; hence, $X1Y1 = X2Y2$. Following the same approach previously used to examine the interaction of a scorpion toxin with the Shaker potassium channel (13), we define the coupling coefficient, Ω , as

$$\Omega = \frac{X1}{X2} = \frac{Y2}{Y1} = \frac{EC_{50}^{WT} \times EC_{50}^{Y72H/W288H}}{EC_{50}^{Y72H} \times EC_{50}^{W288H}} \quad (\text{Eq. 1})$$

If the two mutated residues are independent of one another, then Ω will be unity. If the residues interact and the mutations alter their interaction, then Ω will deviate from unity.

The concentrations of protons to achieve half-maximal activation, expressed in mol, were 2.19×10^{-7} for WT, 3.72×10^{-6} for Y72H, 2.06×10^{-6} for W288H, and 3.72×10^{-6} for the double mutant Y72H/W288H. Introducing these numbers in the above equation gives a value for Ω of 0.1, significantly different from unity.

We could not apply double-mutant cycle analysis to the pair of mutations Y72R and W288R because the latter did not respond to pH as low as 4.0, suggesting that the mutation mark-

edly decreased proton sensitivity of ASIC1-W288R, shifting the pH_{50} into a more acidic range.

Proline 287 in the Loop Containing Trp-288 Is Essential for ASIC1 Function—The tip of subdomain F forms a sharp loop that directs Trp-288 downward and toward Tyr-72. Most residues in this loop are conserved in all ASIC, specifically Leu-284, Pro-285, and Pro-287 (indicated in red, Fig. 1*b*). The functional effect of mutations of each of these conserved residues is shown in Table 1. Substitution of Leu-284 by alanine was functional, but proline in the same position abolished current. Substitutions of Pro-287 by Ala or Gln also abolished proton-activated currents despite good levels of expression at the cell surface (Fig. 2*D*).

The high sensitivity to mutagenesis of this loop is unexpected given that the side chains of these residues, with the exception of Trp-288, are not engaged in interactions with

other amino acids but are mostly surrounded by water. This observation rather suggests that the importance of the proline rests on correctly positioning the aromatic 288 in order to interact with the one in position 72. This occurs by the unique property of proline to bend the backbone of the protein, thereby changing the curvature of the loop or by *cis-trans* isomerization (14). In either case the orientation of the aromatic ring in position 288 would be altered by the absence of proline in 287.

The Linker Tethering Subdomain F to the Body of the Extracellular Domain Decreases Proton-activated Currents and Slows Activation of ASIC1—Residue Pro-365 is conserved in all the ASIC channels. It is located in the short linker connecting subdomain F to the rest of the extracellular domain (Fig. 1*a*); thereby it is poised to sense conformational changes that may displace subdomain F during the gating process. ASIC1 channels bearing the mutation P365A were functional but exhibited marked changes in properties; peak currents elicited by protons were small (wild type 12 ± 5 versus $1.5 \pm 0.4 \mu\text{A}/\text{oocyte}$), and kinetics of activation were slow (wild type 20 ± 5.4 versus $2.75 \pm 1.2 \text{ s}^{-1}$) as well as the desensitization rate (wild type 0.50 ± 0.05 versus $0.18 \pm 0.08 \text{ s}^{-1}$). Last, the rate of recovery from desensitization was slower than in wild type channels (Fig. 2*C*); indeed, recovery from desensitization was never complete but declined progressively until the currents disappeared even after increasing the interval between stimuli for a period as long as 5 min (Fig. 2*F*). These changes in kinetics are consistent with subdomain F being part of the transduction mechanism that translates binding of protons to opening and closure of the pore.

Negatively Charged Residues in the Putative Proton Sensor Change the pH_{50} and Desensitization Rate of ASIC1—The residues Glu-346 and Asp-350 in subdomain F directly face Asp-

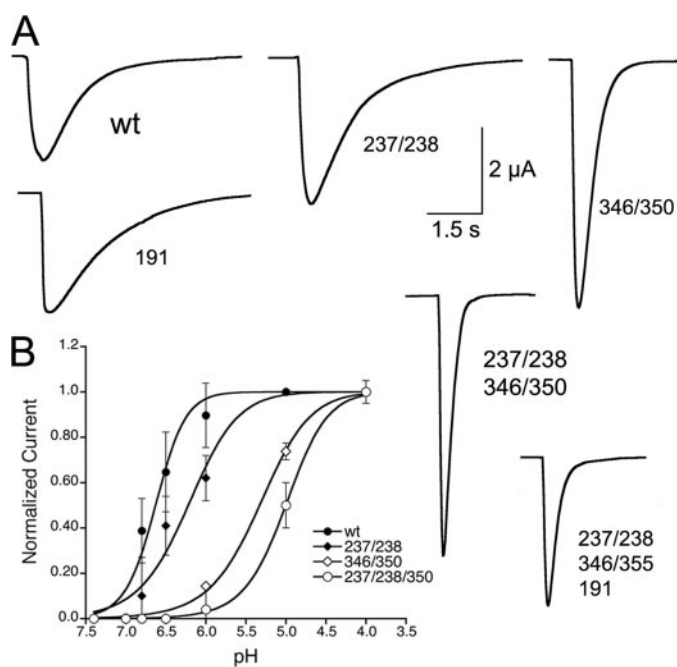


FIGURE 4. Functional effects of amino acid substitutions in putative proton sensor. *A*, representative current traces of channels with additive substitutions of charged residues in the proton sensor for alanine elicited by pH 6.0. Rates of desensitization λ_d (s^{-1}) at pH 6.0 were: WT = 0.45 ± 0.08 ; R191A = 0.47 ± 0.11 ; D237A/E238A = 0.50 ± 0.09 ; E346A/D350A = 2.5 ± 0.1 ; D237A/E238A/E346A/D350A = 2.43 ± 0.1 ; D237/E238/E346A/D350A/R191A = 2.8 ± 0.1 . *B*, pH response curves. Lines are fits to the Hill function. $n = 6-8$ oocytes per data point.

238 and Glu-239 in subdomain E and together with Arg-191 in subdomain D form a cluster of charges at the surface of each subunit that was originally proposed to constitute the proton sensor (Fig. 1*a*). Substitutions of Glu-346 and Asp-350 by Ala maintained functional channels, but the rates of desensitization became faster (wild type $0.48 \pm 0.08 s^{-1}$ versus D350A $2.3 \pm 0.07 s^{-1}$), and the apparent affinity for protons decreased (wild type pH_{50} 6.8 ± 0.5 versus D350A pH_{50} 5.5 ± 0.6) (Fig. 4, *A* and *B*). Removal of the remaining charged residues, Asp-238, Glu-239, and Arg-191, further shifted the apparent pH_{50} of activation toward more acidic pH, but mutant channels still retained the property of being activated by protons. Together these results indicate that protonation of residues in the intrasubunit interface of subdomains F and D affects the conformational changes of activation and, therefore, contributes to the apparent affinity for protons. Although each of these residues plays a role in defining the functional properties of wild type ASIC1, none singly nor all five together are sufficient to confer proton sensitivity to the channel (8, 15); other residues must participate in making the "proton sensor."

DISCUSSION

This study shows that residues Tyr-72 and Trp-288 are essential for proton gating of the ASICs. As any combination of aromatic residues (Trp, Tyr, Phe, or His) when present in these two positions was able to keep ASIC responsive to protons, it is reasonable to conclude that the aromatic side chains in positions 72 and 288 interact and that the interaction is essential to preserve functional channels. All other mutants carrying non-aromatic residues, with the exception of Arg in position 72, did

not open with a pH as low as 4.0, consistent with the notion that an aromatic-aromatic interaction, also termed $\pi-\pi$ interaction, provides the lowest energy barrier between two functional states. Further evidence comes from double cycle mutant analysis conducted with channels having His in positions 72 and 288. These channels were functional but had reduced apparent affinity for protons. Of significance, the effect of the mutations on the apparent pH_{50} was not additive, consistent with functional interaction between residues 72 and 288. The finding that His mutants exhibited lower affinity for protons indicates that the $\pi-\pi$ interaction comprising imidazole rings is not as favorable as when it occurs between Tyr-, Phe, or Trp. We, therefore, interpret the absence of current when other residues occupy positions 72 or 288 to be the result of a shift in the apparent pH_{50} toward a very acidic range (lower than pH 4.0) because of a high energy barrier between states. Such a shift prevented reaching enough low pH to open the mutant channels without damaging the oocytes. This interpretation is favored over disruption of channel structure or misfolding induced by the mutations because of robust surface expression of mutant channels, functional channels carrying arginine (Y72R) despite marked differences in properties between the side chain of arginine and aromatic amino acids, and because the corresponding mutations in ENaC, a channel structurally related to ASIC but not gated by protons, retained function.

Aromatic-aromatic interactions contribute to maintaining tertiary and quaternary structure of proteins by stabilizing contacts between subdomains and between proteins within a complex. Aromatic-aromatic interactions are characterized by a competition between the stacked and the T-shaped geometries, the latter being more frequent in proteins (16). In the T-shape structure the planes of the ring are perpendicular to each other, and in the intermediate stacked, "edge-displaced," the ring planes are parallel-displaced. This competition is strongly affected by polarity of the environment and the ability of the surrounding solvent to form hydrogen bonds. In the crystal structure of cASIC1, Tyr-72 and Trp-288 adopt a T-shape structure; whether this geometry changes in the open, closed, and desensitized states is not known, although the binding energy differences for Tyr/Trp pair would be in the order of 1 kcal/mol going from T-shaped to intermediate stacked and 1.6 kcal/mol to the stacked geometry according to previous calculations (17). These values are in the range of energy change between the open and close conformations of ASIC1.

The observation that pH solutions in the range of 6.0 to 4.0 open the mutant Y72R, but not Y72K or W288R, indicates that Arg in position 72 can functionally replace one of the aromatic rings in the pair. An explanation for such an unexpected finding is that the positively charged side chain of Arg can interact with the aromatic ring in 288, replacing the $\pi-\pi$ interaction for a cation- π interaction (18). In the cation- π interaction, side chains of aromatic amino acids provide a surface of negative electrostatic potential that can bind to cations through a predominantly electrostatic interaction. This is possible only when arginine is in position 72 because here the arginine side chain would point to the aromatic ring, whereas arginine in position 288 would point its side chain away from Tyr-72 (Fig. 5). The preference of arginine over lysine can be explained by the fact

Tyr-72 and Trp-288 Are Required for ASIC Function

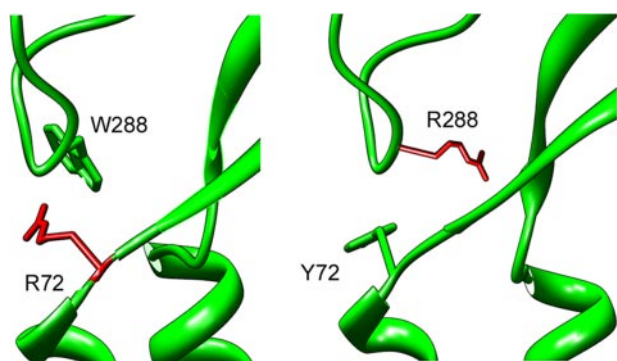


FIGURE 5. Representation of Arg in positions 72 and 288 in ASIC1. The figure was obtained by substituting Tyr-72 and Trp-288 in the crystal structure of chicken ASIC1 by Arg to illustrate the relative position of the positively charged side chain with respect to the opposite aromatic residue.

that the face of the guanidinium ion of arginine is to some extent hydrophobic, thereby preferred by the innately hydrophobic aromatic (19).

Additional evidence for the importance of correct positioning of the aromatic rings in the Tyr-72/Trp-28 pair was provided by mutations in the loop holding Trp-288. This loop exhibits a tight bend in the crystal structure because of the presence of several conserved prolines that when mutated also abolish current, suggesting that the curvature of the loop or *cis-trans* isomerization of the prolines (14) positions the aromatic ring of amino acid 288 to allow interaction with the aromatic at position 72.

The prediction that Trp-288 may move together with subdomain F during the gating process was supported indirectly by changes in apparent pH_{50} and kinetics induced by point mutations in sites of contact of subdomain F with the rest of the ECD; *i.e.* the interface of subdomains F and E; the first through carbonyl-carboxylate interactions of residues Asp-346 with Asp-238 and Asp-350 with Glu-239 and the second through Pro-365, in a hinge-like structure connecting subdomain F to the rest of the ECD. Furthermore, our findings are in agreement with the recently published molecular dynamic analysis of cASIC1 (20). A simulation in which Ca^{2+} ions bound to the proton sensor were displaced by protons unveil conformational changes in subdomain F (thumb domain) that were largest in the loop containing Trp-288. Our results are somewhat reminiscent of the Cys-loop ligand-activated receptors, where the importance of the interface of the extracellular with the transmembrane domain in communicating conformational changes

initiated in the ligand binding site to the gate of the pore has been demonstrated (21).

We conclude that an aromatic interaction between Tyr-72 and Trp-288 is required for conferring proton sensitivity to the ASICs, most likely by stabilizing a conformation that promotes channel opening. Residues in the putative proton sensor and in the tethers that connect subdomain F to the rest of the body of the extracellular domain contribute to move subdomain F; thereby the aromatic ring of Trp-288 is placed in a position that allows it to interact with Tyr-72. Together these findings provide experimental support for the proposal that subdomain F is involved in ASIC1 gating.

REFERENCES

1. Wemmie, J. A., Price, M. P., and Welsh, M. J. (2006) *Trends Neurosci.* **29**, 578–586
2. Zhang, P., and Canessa, C. M. (2002) *J. Gen. Physiol.* **120**, 553–566
3. O'Hagan, R., Chalfie, M., and Goodman, M. B. (2005) *Nat. Neurosci.* **8**, 43–50
4. Lingueglia, E., Champigny, G., Lazdunski, M., and Barbry, P. (1995) *Nature* **378**, 730–733
5. Golubovic, A., Kuhn, A., Williamson, M., Kalbacher, H., Holstein, T. W., Grimmekhuijzen, C. J., and Gründer, S. (2007) *J. Biol. Chem.* **282**, 35098–35103
6. Waldmann, R., Champigny, G., Bassilana, F., Heurteaux, C., and Lazdunski, M. (1997) *Nature* **386**, 173–177
7. Canessa, C. M., Schild, L., Buell, G., Thorens, B., Gautschi, I., Horisberger, J. D., and Rossier, B. C. (1994) *Nature* **367**, 463–467
8. Jasti, J., Furukawa, H., Gonzales, E. B., and Gouaux, E. (2007) *Nature* **449**, 316–323
9. Coric, T., Zheng, D., Gerstein, M., and Canessa, C. M. (2005) *J. Physiol. (Lond.)* **568**, 725–735
10. Hurle, M. R., Tweedy, N. B., and Matthews, C. R. (1986) *Biochemistry* **25**, 6356–6360
11. Perry, K. M., Onuffer, J. J., Gittelman, M. S., Barmat, L., and Matthews, C. R. (1989) *Biochemistry* **28**, 7961–7968
12. Horovitz, A., and Fersht, A. R. (1990) *J. Mol. Biol.* **214**, 613–617
13. Hidalgo, P., and MacKinnon, R. (1995) *Science* **268**, 307–310
14. Lummis, S. C. R., Beene, D. L., Lee, L. W., Lester, H. A., Broadhurst, R. W., and Dougherty, D. A. (2005) *Nature* **438**, 248–252
15. Paukert, M., Chen, X., Polleichtner, G., Schindelin, H., and Gründer, S. (2008) *J. Biol. Chem.* **283**, 572–581
16. Burley, S. K., and Petsko, G. A. (1985) *Science* **229**, 23–28
17. Gervasio, F. L., Chelli, R., Procacci, P., and Schettino, V. (2002) *Proteins* **48**, 117–125
18. Dougherty, D. A. (1996) *Science* **271**, 163–168
19. Dougherty, D. A. (2007) *J. Nutr.* **137**, Suppl 1, 1504–1508
20. Shaikh, S. A., and Tajkhorshid, E. (2008) *Biophys. J.* **95**, 5153–5164
21. Bouzat, C., Gumilar, F., Spitzmaul, G., Wang, H. L., Rayes, D., Hansen, S. B., Taylor, P., and Sine, S. M. (2004) *Nature* **430**, 896–900